Journal Pre-proof

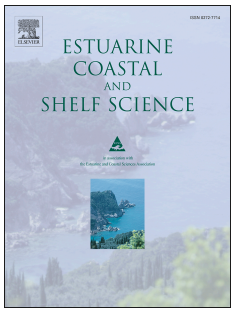

Autochthonous organic matter promotes DNRA and suppresses N_2O production in sediments of the coastal Baltic Sea

Sanni L. Aalto, Eero Asmala, Tom Jilbert, Susanna Hietanen

PII: S0272-7714(21)00222-5

DOI: https://doi.org/10.1016/j.ecss.2021.107369

Reference: YECSS 107369

To appear in: *Estuarine, Coastal and Shelf Science*

Received Date: 14 May 2020

Revised Date: 31 January 2021

Accepted Date: 6 April 2021

Please cite this article as: Aalto, S.L., Asmala, E., Jilbert, T., Hietanen, S., Autochthonous organic matter promotes DNRA and suppresses N_2O production in sediments of the coastal Baltic Sea, *Estuarine, Coastal and Shelf Science* (2021), doi: https://doi.org/10.1016/j.ecss.2021.107369.

Autochthonous organic matter promotes DNRA and suppresses N_2O production in sediments of the coastal Baltic Sea

Sanni L. Aalto[1,2*], Eero Asmala[3], Tom Jilbert[3,4], Susanna Hietanen[3,4]

[1]Department of Environmental and Biological Sciences, University of Eastern Finland, P.O. Box 1627, 70211 Kuopio, Finland

[2]Department of Biological and Environmental Science, University of Jyväskylä, P.O. Box 35, 40014 Jyväskylä, Finland

[3]Tvärminne Zoological Station, University of Helsinki, 10900 Hanko, Finland

[4]Ecosystems and Environment Research Program, Faculty of Biological and Environmental Sciences, 00014 University of Helsinki, Helsinki, Finland

Corresponding author: Sanni L. Aalto, sheaa@aqua.dtu.dk

*current address: Technical University of Denmark, DTU Aqua, Section for Aquaculture, The North Sea Research Centre, P.O. Box 101, DK-9850 Hirtshals, Denmark

Abstract

Coastal environments are nitrogen (N) removal hot spots, which regulate the amount of land-derived N reaching the open sea. However, mixing between freshwater and seawater creates gradients of inorganic N and bioavailable organic matter, which affect N cycling. In this study, we compare nitrate reduction processes between estuary and offshore archipelago environments in the coastal Baltic Sea. Denitrification rates were similar in both environments, despite lower nitrate and carbon concentrations in the offshore archipelago. However, DNRA (dissimilatory nitrate reduction to ammonium) rates were higher at the offshore archipelago stations, with a higher proportion of autochthonous carbon. The production rate and concentrations of the greenhouse gas nitrous oxide (N_2O) were higher in the estuary, where nitrate concentrations and allochthonous carbon inputs are higher. These results indicate that the ratio between nitrate and autochthonous organic carbon governs the balance between N-removing denitrification and N-recycling DNRA, as well as the end-product of denitrification. As a result, a significant amount of the N removed in the estuary is released as N_2O, while the offshore archipelago areas are characterized by efficient internal recycling of N. Our results challenge the current understanding of the role of these regions as filters of land-to-sea transfer of N.

Keywords: denitrification; DNRA; DOM; estuary; N_2O; sediment organic matter

1 Introduction

Coastal systems are transitional zones where riverine freshwater mixes with saline seawater. They are important hot spots in the nitrogen (N) cycle, as N transformations in coastal ecosystems regulate the amount of land-derived N reaching the open sea (Bouwman et al., 2013). Various coastal processes, including assimilation to biomass and subsequent microbial degradation of organic matter, modulate land-to-sea transfer of N. Crucially, N may be removed from biogeochemical cycling in estuaries by a sequence of sedimentary microbial processes terminating in denitrification, which releases dinitrogen gas (N_2) into the atmosphere. Denitrification is a critical part of the 'coastal filter'; the set of biogeochemical processes regulating the impact of riverine nutrient inputs on coastal eutrophication (Asmala et al., 2017).

Denitrification rates in coastal environments depend on nitrate concentrations, which typically decrease from near-shore to offshore areas (Asmala et al., 2017). However, heterotrophic denitrification also depends on the presence of bioavailable organic carbon (OC) in coastal sediments (Hellemann et al., 2017; Hietanen and Kuparinen, 2008). Higher OC bioavailability has been suggested to promote denitrification in freshwater stream sediments (Barnes et al., 2012; Stelzer et al., 2014), raising the question of whether the same is true in coastal marine systems. Coastal systems often display strong gradients in both nitrate concentrations, and in sedimentary OC sources and characteristics, with distance away from river mouths. Typically, the relative amount of terrestrial OC in sediments decreases gradually along the coastal salinity gradient, while the amount of fresh, autochthonous phytoplankton-derived OC increases (Fellman et al., 2011; Goñi et al., 2003; Spencer et al., 2007). Combined, these observations suggest that coastal nitrate removal efficiency through denitrification could be related to the availability of both nitrate and bioavailable OC (Asmala et al., 2017).

The balance in the availability of nitrate and bioavailable carbon may also influence rates of alternative nitrate reduction pathways. Heterotrophic dissimilatory nitrate reduction to ammonium (DNRA), which retains N as biologically reactive ammonium in the aquatic system (e.g., Giblin et al., 2013), is the prominent pathway under conditions of high OC availability relative to nitrate (Hardison et al., 2015; Kraft et al., 2014). This phenomenon may occur because under nitrate-limited conditions, DNRA makes more efficient use of the available electron acceptors (6 electrons transferred per mole of N reduced compared to 3 for denitrification), and therefore maximizes entropy production (Algar and Vallino 2014). Furthermore, OC composition is as important as OC availability in controlling the nitrate reduction end-product (Carlson et al., 2020). From this, it follows that the importance of DNRA in net nitrate reduction may increase towards the open sea where terrestrial influence decreases (lower nitrate

and higher bioavailable carbon concentrations). Indeed, high contributions of DNRA to total nitrate reduction were recently observed in the Baltic Sea offshore region (Hellemann et al., 2020) and in Australian estuaries (Kessler et al., 2018). Therefore, outer coastal areas may recycle nitrate more efficiently than remove it, in comparison with near-shore areas with a lower bioavailable OC to nitrate ratio, which favours denitrification.

Incomplete denitrification leads to the production of nitrous oxide (N_2O). The proportion of N_2O production from total denitrification can increase with DIN concentrations (Murray et al., 2015), and decrease with increased bioavailable carbon (Zhao et al., 2014). This suggests that among other variables (e.g. oxygen, temperature, salinity, and rates of nitrogen fixation and nitrification; Foster and Fulweiler, 2016; Silvennoinen et al., 2008; Zhao et al., 2014), OC bioavailability is an important factor controlling denitrification-derived N_2O production in coastal ecosystems, and N_2O production the rates may be higher in near-shore estuarine environments with low amounts of bioavailable OC and high nitrate concentrations. Hence, OC characteristics and especially bioavailability may play a key role in many aspects of coastal sedimentary N cycling. These factors must be deconvolved from the effects of nitrate gradients to properly understand the coastal N cycle.

The overall bioavailability of aquatic OC can be assessed with optical proxies of dissolved organic matter (DOM), derived from the absorbance and fluorescence properties of the colored dissolved organic matter (CDOM) (Asmala et al., 2013). A range of optical proxies (e.g. the humification index (HIX) and the index of recent autochthonous contribution (BIX)) have been derived to characterize the DOM pool (Huguet et al., 2009; Murphy et al., 2008). We assume DOM in sediment porewaters to reflect the broad overall organic matter composition of sediments, and optical analysis of porewater DOM composition provides a tool for characterizing the source and bioavailability of sedimentary carbon. Porewater DOM characterization potentially provides additional information to traditional approaches such as C/N ratios or $\delta^{13}C$ of bulk organic matter.

Here, we investigate the combined influence of nitrate availability and organic matter composition on nitrate reducing processes in coastal sediments in the northern Baltic Sea. The Baltic is a semi-enclosed shallow brackish water basin with significant anthropogenic N loading. In 2010, the total N load to the Baltic was 977 000 tons, of which 758 000 tons was waterborne (Helcom 2015), yielding a waterborne N load from the catchment of 0.44 tonnes/km^2. The Baltic Sea coastal zone (29% of total Baltic Sea area) was estimated to remove 16% of land-derived N inputs, the N removal efficiency varying between different types of coastal ecosystems (Asmala et al. 2017). Denitrification dominates N_2 production in Baltic Sea coastal ecosystems, with anammox playing only a minor role (Bonaglia et al., 2014; Hietanen, 2007; Thamdrup and Dalsgaard, 2002). Knowledge on the balance between

denitrification and DNRA is limited for this region, but results from an anthropogenically impacted Baltic Sea estuary suggest that denitrification is the main process (Bonaglia et al., 2014) due to the high DIN availability, and that the contribution of DNRA increases to 30-50% of total nitrate reduction in the offshore region (Hellemann et al., 2020). The limited data from oligotrophic coastal sediments of the Baltic Sea, where availability of labile organic carbon limits the denitrification process, also indicate that N_2O production from benthic denitrification is low ($N_2O:N_2$ <0.02) (Hellemann et al., 2017).

In this study, we measured porewater DOM characteristics, nitrous oxide concentrations, and N processes along a gradient encompassing near-shore (estuary) and offshore archipelago stations in a coastal region of the Baltic Sea to examine the effects of both nitrate availability and OC characteristics on nitrate reduction processes. We hypothesized that higher nitrate availability and terrestrial dominance of the carbon pool (i.e. low quantities of bioavailable carbon compared to nitrate) would promote denitrification and possibly N_2O production at the near-shore estuarine stations. Conversely, we hypothesized that the significance of DNRA as a nitrate reduction process would increase at the offshore archipelago stations due to a higher amount of bioavailable carbon and/or lower nitrate concentrations.

2 Materials and methods

2.1 Study area, sampling, and water column analyses

The study was conducted in the Finnish coastal area of the Gulf of Finland, Baltic Sea. Pohjanpitäjänlahti is a long and narrow embayment that receives freshwater input from the river Mustionjoki and brackish water input from the adjacent coastal archipelago of the Baltic Sea (Fig. 1). A shallow (2-3 m) sill area, with a dredged 6 m channel through it, separates the estuary from the offshore region connecting to the open Baltic Sea, limiting the water exchange between the estuary and the offshore region. The inner basin is salinity-stratified, with a pronounced pycnocline at 10-15 m water depth, which leads to seasonal hypoxia in summer and autumn. Inflows of brackish water over the sill usually occur in late autumn – early winter, leading to temporary ventilation of the basin (Malve et al., 2000). The adjacent offshore region experiences temperature stratification in summer, leading to the development of hypoxia in isolated areas. However, much of that remains oxic throughout the annual cycle due to sufficient vertical mixing and exchange of water masses. The catchment of the Mustionjoki has a large proportion of lakes (11%; Mattsson et al., 2005) and several hydropower plants regulating the flow. This characteristic leads to extensive processing of the riverine nutrients and organic matter already within the lotic system and relatively low area-specific loading of organic carbon to the estuary (Räike et al., 2012).

To monitor water column N_2O concentrations, water column sampling was conducted at stations P4 ("estuary", see Fig. 1) and STF ("offshore archipelago") at 5 m depth intervals using a 5L Limnos sampler on multiple occasions during 2015-2017. Subsamples for determination of dissolved N_2O were collected in triplicate by filling 60mL plastic syringes directly from a Limnos water sampler on board. In the laboratory, the water volume in the syringe was reduced to 30 mL, and 31mL of 5.0 purity N2 gas was injected to create a headspace. Syringes were left at 20 C for 30 min and then vigorously shaken for 3 min, after which 25mL of the headspace was injected into a pre-evacuated 12mL gastight glass vial (LabCo Exetainer model 839W). Nitrous oxide concentrations in the headspace were determined using an Agilent Technologies 7890B gas chromatograph equipped with electron capture detector (ECD) and the results calculated as in Myllykangas et al. (2017).

Sampling was carried out at two stations in the estuary (stations P1 and P4) on 6th of June 2017 and 15th–16th of August 2017 and at two stations in the offshore archipelago region (stations P10 and STF; Fig. 1) only on 15th–16th of August 2017. Sampling occasions were chosen to represent situations with high (June) and low (August) amount of fresh, recently deposited phytoplankton-derived material on the sediment surface (Heiskanen and Kononen, 1994). Temperature, salinity and oxygen were determined using a YSI CTD equipped with an optical oxygen sensor. Sediment cores were collected using a Gemax twin sampler (core diameter 9 cm, length of a core 30 - 50 cm) from each sampling station. Water samples were collected using a 5L Limnos water sampler from 1 m depth to 1 m above the sediment at 2-5 m intervals, and from the overlying water of the sediment cores. Oxygen samples for Winkler titration (150 ml) were treated immediately with fixing reagents and analyzed the following day. Dissolved inorganic nitrogen (ammonium, nitrite and nitrate) samples were collected in acid-washed plastic bottles, filtered through 0.2µm polycarbonate filters and stored dark at 4°C. Concentrations were measured using a discrete photometric analyzer (Thermo Scientific Aquakem 250) the following day. Theoretical 3-sigma detection limits were as follows: ammonium 0.11 µM, nitrate and nitrite 0.08 µM.

Figure 1. (left) Sampling locations in the Pohjanpitäjänlahti system on the Finnish coast of the Gulf of Finland, northern Baltic Sea. Stations P1 and P4 are classified as "estuary" stations, while P10 and STF are classed as "offshore archipelago". The Mustionjoki river discharges into the Pohjanpitäjänlahti estuary close to station P1. (right) Bathymetric detail of the transect through the sampling locations, showing typical salinity distribution (data shown here from June 2015, redrawn from Jilbert et al., 2018). A shallow sill close to the city of Ekenäs restricts exchange of brackish deeper waters between the offshore archipelago and estuary.

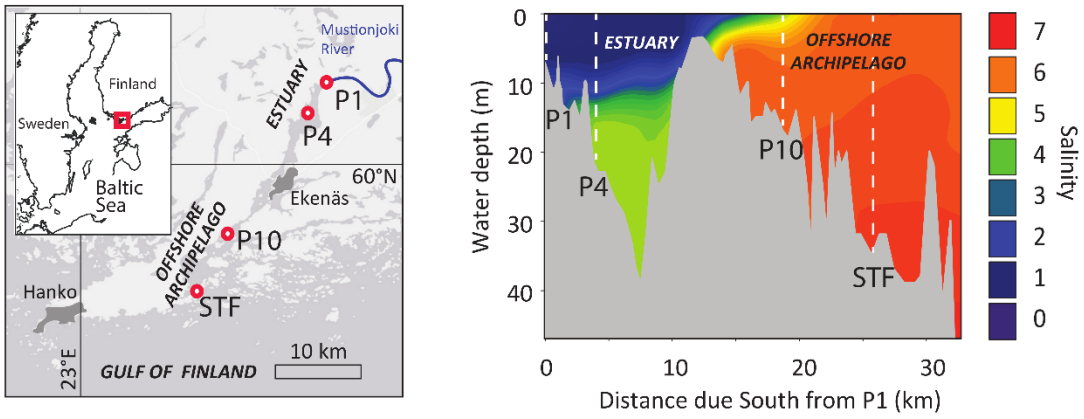

2.2 Sediment and porewater analyses

Sediment cores were collected using a Gemax twin sampler (core diameter 9 cm, length of core 30 - 50 cm) from each sampling station. Sediment water content and porosity were determined from the upper portion of each core (0–6 cm) (Burdige, 2006). Sediment total C and N content (%C, %N) of the upper portion was determined by Thermal Combustion Elemental Analysis (TCEA) at Tvärminne Zoological Station with precision and accuracy of < 2.5% RSD. Sedimentary inorganic carbon and nitrogen are assumed insignificant in this setting, hence $\%C_{tot}$ and $\%N_{tot}$ are assumed equal to organic carbon and nitrogen, respectively ($\%C_{org}$ and $\%N_{org}$).

Porewater DOC and CDOM samples were taken from the surface sediment layer (0-1 cm) of three replicate cores. In the laboratory, pore water was extracted with centrifuging (1500 rpm for 10 min), and filtered through a combusted (4 h 450 °C) glass fiber filter (47 mm, VWR collection GF/F). DOC concentration in porewaters was measured with a Shimadzu TOC-V_{CPH} analyzer. The detection limit for DOC analysis was 40 µmol L^{-1}. CDOM absorption was measured using a Shimadzu 2401PC spectrophotometer with 1 cm quartz cuvette over the spectral range from 200 to 800 nm with 1 nm intervals. Ultrapure water served as the blank for all samples. Excitation-emission matrices (EEMs) of fluorescent DOM (FDOM) were measured and corrected as in Asmala et al., (2018). For assessing the terrestrial signature of the porewater DOM, fluorescence peaks (peaks A, C, M, and T; Coble, 1996), humification index (HIX; Zsolnay et al., 1999) and biological index (BIX; Huguet et al., 2009) were calculated from the measured and corrected EEMs. Processing of the EEMs was done using the eemR package for R software (Massicotte, 2018).

2.3 Sedimentary nitrogen process rates

Samples for benthic nitrate reduction rate measurements (n=8 per sampling station) were collected into acrylic cores (Ø 2.3 cm, length 15 cm), which were pushed gently into the sediment so that 1/3 of each core was filled with sediment and the rest with overlying water, capped and placed in a

water bath at *in situ* temperature. The four cores were immediately enriched with ^{15}N-labelled nitrate to a final concentration of 100 µM ^{15}N-NO_3^- ($K^{15}NO_3$ Sigma Aldrich, 98% ^{15}N-atm), closed and incubated under stirring at *in situ* temperature in dark for 3-4 h. Enrichment with 200 µM ^{15}N-NH_4^+ ($^{15}NH_4Cl$ Cambridge Isotope Laboratories, 99% ^{15}N-atm; 4 replicate cores) was used to exclude anammox and measure nitrification (data not shown). After incubation, sediment and overlying water in the samples were mixed and 12 mL subsamples were transferred into gas-tight glass vials (Labco Exetainer model 739W) with 0.5 mL $ZnCl_2$ (100 % w/v, Merck) after a brief sediment settling period. Isotopic composition of N_2 and N_2O was analysed with a TraceGas preconcentrator system interfaced with an IsoPrime 100 continuous flow isotope ratio mass spectrometer (CF-IRMS; Isoprime Ltd, Cheadle Hulme, UK) at the Department of Environmental Sciences, University of Jyväskylä, Finland as in Hellemann et al., (2017). The detection limits were 320 nmol L^{-1} for $^{29}N_2$, 11 nmol L^{-1} for $^{30}N_2$, 397 pmol L^{-1} for $^{45}N_2O$, and 322 pmol L^{-1} for $^{46}N_2O$.

The remaining $^{15}NO_3^-$-enriched slurry was mixed again, and 20 mL samples for $^{15}NH_4^+$ analysis were collected into 50 mL centrifuge tubes, treated with 1 mL of $ZnCl_2$, and frozen immediately. Before $^{15}NH_4^+$ analysis, NH_4^+ attached to the sediment particles was desorbed using KCl extraction. The isotopic composition of NH_4^+ in the samples was analyzed after conversion to N_2 using alkaline hypobromite iodine solution (Risgaard-Petersen et al., 1995) as in Hellemann et al., (2020). A standard series of $^{15}NH_4^+$ (5; 10; 15 µM, 5% ^{15}N-atm from $^{15}NH_4Cl$ Cambridge Isotope Laboratories, 98% ^{15}N-atm) was prepared, treated and analyzed parallel with samples to calculate conversion efficiency and ^{15}N recovery, which was > 85 %.

The N_2 and N_2O producing denitrification rates were calculated from the production rates of $^{29}N_2$, $^{30}N_2$ and $^{45}N_2O$, $^{46}N_2O$), and partitioned to denitrification based on water column nitrate (D_w) and coupled nitrification-denitrification (D_n) (Nielsen, 1992). DNRA rates were calculated from the production rates of $^{15}NH_4^+$ and the production rates of $^{29}N_2$, $^{30}N_2$ and $^{45}N_2O$, $^{46}N_2O$ in the same incubation cores according to Christensen et al., (2000). It was assumed that DNRA takes place in the same layers as denitrification, meaning that the ^{15}N labeling of NO_3^- reduced to ammonia equals the ^{15}N labeling of NO_3^- reduced to N_2/N_2O. Total N_2 production ($\sum N_2$) was calculated as $\sum N_2 = D_w\_N_2 + D_n\_N_2$ and total N_2O production ($\sum N_2O$) as $\sum N_2O = D_w\_N_2O + D_n\_N_2O$. The total denitrification was then defined as $\sum N_2 + \sum N_2O$ and total nitrate reduction as $\sum N_2 + \sum N_2O$ + DNRA. The hourly rates were scaled to day by multiplying with 24h. The N_2O produced in coupled nitrification-denitrification was divided into the rate of N_2O produced in the nitrification stage and the denitrification stage of the coupled nitrification-denitrification according to Dong et al., (2006).

2.4 Statistical analysis

The data analysis was conducted using R (version 3.6.3; R Core Team, 2020). The differences in the porewater DOM characteristics, and N processes between estuary and offshore archipelago region were examined with one-way ANOVA, or if the assumptions on the normality and equal variances were not met, with Mann-Whitney U test. The relationship between DOM variables and N processes were examined with Pearson correlation analysis, and relative DNRA (%DNRA) and N_2O (%N_2O) and DOC and bioavailable carbon fraction (protein-like DOM fluorescence) were further examined with linear regression.

3 Results

3.1 Hydrography

In both estuary and offshore archipelago, the water column was well oxygenated during the sampling campaigns despite being stratified, with a thermocline present at all stations between 3.5-10 m depth (Table 1; Suppl. Fig. 1). At the estuary stations, closer to the direct influence of the Mustionjoki River, a pronounced halocline was present (Suppl. Fig. 1).

Table 1. Temperature (T), salinity, oxygen concentration (O_2), and DIN concentrations (NO_x^-, NH_4^+) in near-bottom water and sediment C:N at the estuary and offshore archipelago sampling stations.

	Station	Sampling time	T °C	salinity	O_2 µM	NO_x^- µM	NH_4^+ µM	C:N
Estuary	P1	June 2017	5.8	4.0	234	11.1	0.7	18.7
	P4	June 2017	3.3	5.1	236	13.0	1.5	12.4
	P1	August 2017	13.8	3.3	155	1.7	3.2	21.6
	P4	August 2017	4.7	5.0	126	14.1	6.1	12.7
Offshore archipelago	P10	August 2017	10.1	6.2	176	1.6	5.8	11.2
	STF	August 2017	8.8	6.4	216	1.4	4.0	10.1

3.2 Dissolved inorganic nitrogen and nitrous oxide

The near-bottom combined nitrite+nitrate (NO_x^-) concentrations decreased as expected from near-shore estuary to offshore archipelago stations. At the estuary stations P1 and P4, near-bottom NO_x^-

concentrations varied between 3-14 µM (Table 1; Suppl. Fig. 2). Near-bottom NO_x^- concentrations were consistently low (≤ 1.6 µM) at the offshore archipelago stations P10 and STF. Near-bottom ammonium (NH_4^+) concentrations (1-6 µM) were similar at all sampling stations. Dissolved nitrous oxide (N_2O) concentrations were consistently high (25-50 nM at P4, Fig. 2) below the halocline in the estuary. Surface waters at the offshore archipelago stations, P4 and STF, and deeper waters at STF, had lower N_2O concentrations (10-30 nM), except for a high value in the surface waters of P4 under ice cover in March 2017.

Figure 2. Nitrous oxide (N_2O) concentration in water column above (blue triangles) and below halocline (red circles) between April 2015 and August 2017 at the near-shore estuary (station P4) and offshore archipelago (station STF) stations. Points indicate mean value and error bars ± 1 standard deviation. Number of observations per each mean value in the figure ranges between 3 and 24, the median number of observations being 10.

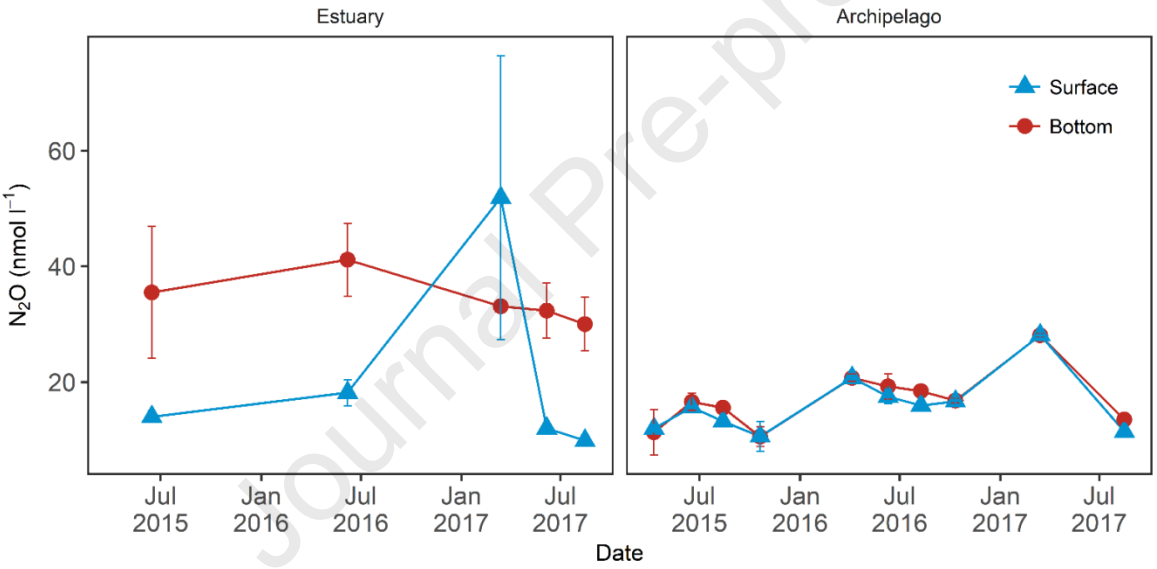

3.3 Organic carbon source proxies

All the sampled sediments were muddy, with surface (0-1 cm) porosities ranging from 0.94 to 0.97. Sediment C:N ratio decreased from the estuary (16 ± 5) to the offshore archipelago stations (11 ± 1) (Table 1). The amount of bulk dissolved organic matter in the porewater, as indicated by the DOC concentration, was almost twice as high at the estuary stations as at the offshore archipelago stations (Fig. 3a). The ratio (mean ± SD) between DOC concentrations in the uppermost sediment layer (0-1 cm) and near bottom NO_x (DOC:NO_x^-) was 2.5 ± 2.9 at the estuary stations and 4.8 ± 1.3 at the offshore archipelago stations. Organic matter characteristics were on average more terrestrial-like at the estuary than at the offshore archipelago stations (one-way ANOVA, $p < 0.05$), as indicated by optical proxies: higher CDOM absorption at 254 nm ($a_{(CDOM254)}$), DOC-specific UV absorbance ($SUVA_{254}$), humic- and protein-like DOM fluorescence (peak C and T, respectively) and higher

humification index (HIX). Also, at the offshore archipelago stations, UV absorption slope ($S_{275–295}$) and biological index (BIX) were higher than at the estuary stations ($p < 0.05$; Fig. 3), indicating higher contribution of autochthonous bioavailable carbon with smaller molecular size.

3.4 Nitrogen transformation rates in estuary and offshore archipelago sediments

All nitrate reduction rates varied substantially between the sampling stations, as both the highest and lowest rates were measured at the estuarine stations (Fig. 4, Suppl. Fig. 3). Total denitrification ($\sum N_2 + \sum N_2O$) rates and total nitrate reduction ($\sum N_2 + \sum N_2O$ + DNRA) rates did not differ significantly between the estuary and offshore archipelago stations (Mann-Whitney U test, $p > 0.05$, Fig. 4, Suppl. Fig. 3). No anammox was detected (data not shown). Denitrification rates based on water column nitrate ($D_w\_N_2$, $D_w\_N_2O$) were higher at the estuary stations ($D_w\_N_2$: one-way ANOVA, $p = 0.004$; $D_w\_N_2O$: $p < 0.001$), but the coupled nitrification-denitrification process rates ($D_n\_N_2$, $D_n\_N_2O$) were dominant and equal between the estuary and offshore archipelago stations ($p > 0.05$, Fig. 4, Suppl. Fig. 3). Similarly, DNRA rates based on water column nitrate ($DNRA_w$) were higher at the estuary stations ($p = 0.006$), while total DNRA rates ($p = 0.024$) and the proportion of DNRA of total nitrate reduction (%DNRA; $p = 0.03$) and nitrification-fed DNRA ($DNRA_n$; $p = 0.003$) rates were higher at the offshore archipelago stations (Fig. 5, Suppl. Fig. 3). The proportion of N_2O produced in nitrate reduction ($\%N_2O$) as well as the proportion of N_2O produced from the denitrification stage of coupled nitrification-denitrification were higher at the estuary stations than at the offshore archipelago stations ($\%N_2O$: $p < 0.001$, $\%N_2O$ from denitrification: $p = 0.006$), being especially high at P4 in August (Fig. 5). Significant relationships between organic carbon characteristics (source proxies) and both %DNRA (decreasing with higher terrestrial OM share) and $\%N_2O$ (increasing with higher terrestrial OM share) were observed (Suppl. Table 1), while no relationship was found with total denitrification rates. Notably, the variance of either %DNRA or $\%N_2O$ was not explained by bulk carbon concentration (DOC) (Fig. 6a–b). Rather, protein-like DOM fluorescence (a common proxy for biologically labile organic carbon) had a strong negative relationship with %DNRA and strong positive relationship with $\%N_2O$ (Fig. 6c–d).

Figure 3. Porewater (0–1 cm) DOM quantity and quality characteristics at the estuary stations in June (left orange bar, n = 6) and August (right orange bar, n = 6) and at the offshore archipelago stations in August (n = 6): a) dissolved organic carbon (DOC), b) CDOM absorption coefficient at 254 nm ($a_{(CDOM254)}$, c) humic-like DOM fluorescence (Peak C), d) protein-like DOM fluorescence (Peak T), e) CDOM spectral slope between 275–295 nm ($S_{275–295}$), f) DOC-specific UV absorbance at 254 nm ($SUVA_{254}$), g) humification index (HIX) and h) biological index (BIX). Mean values ± standard deviation for estuary and offshore archipelago groups are also given. The two groups are significantly different for each variable (one-way ANOVA, $p < 0.05$).

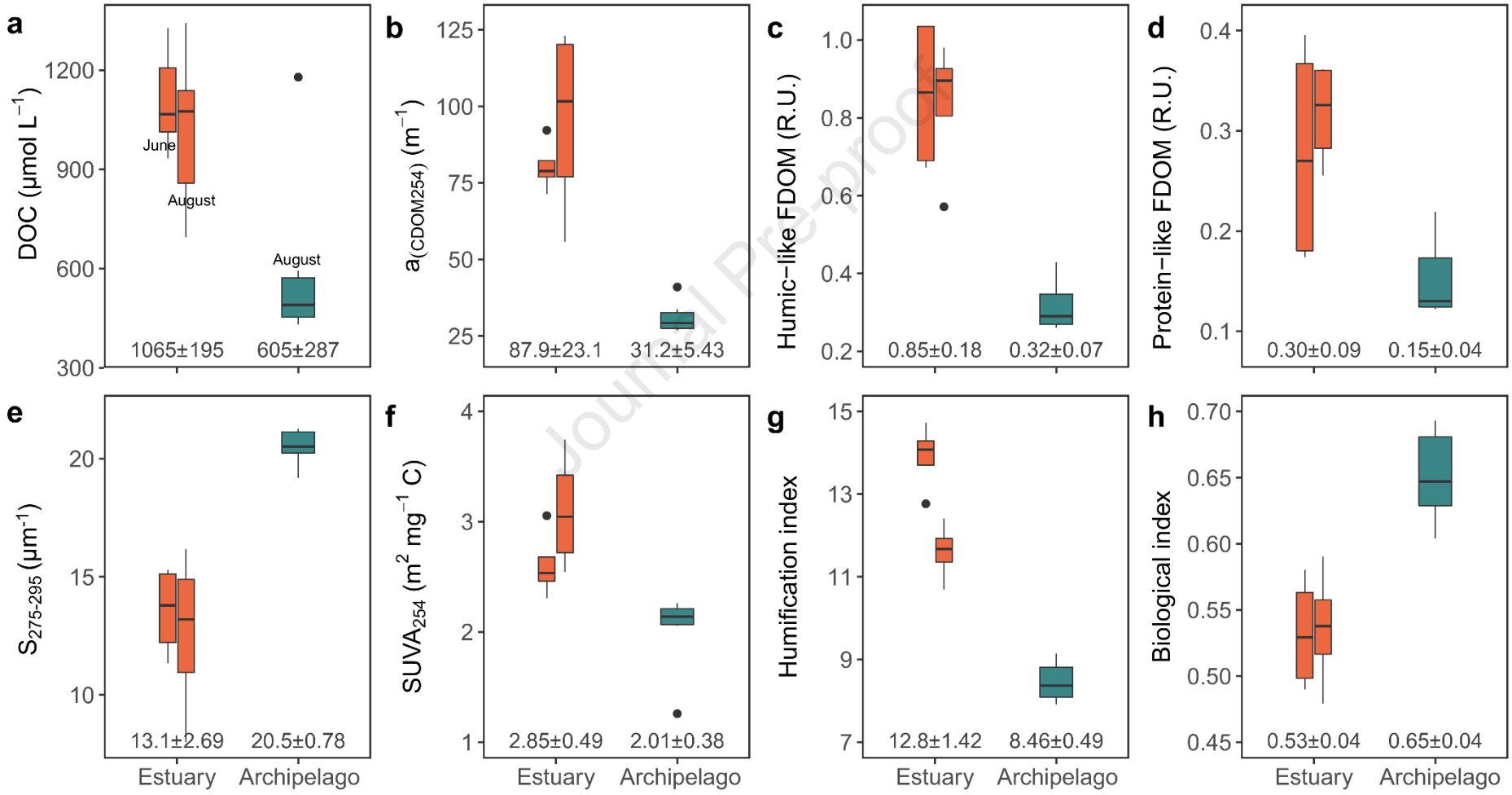

295 Figure 4. DNRA and denitrification rates at the estuary (P1, P4) and offshore archipelago (P10, STF) stations. D_w denotes water column nitrate based process
296 and D_n process based on the nitrate produced through sediment nitrification. Bars represent mean values ± standard error for four sediment core
297 replicates.

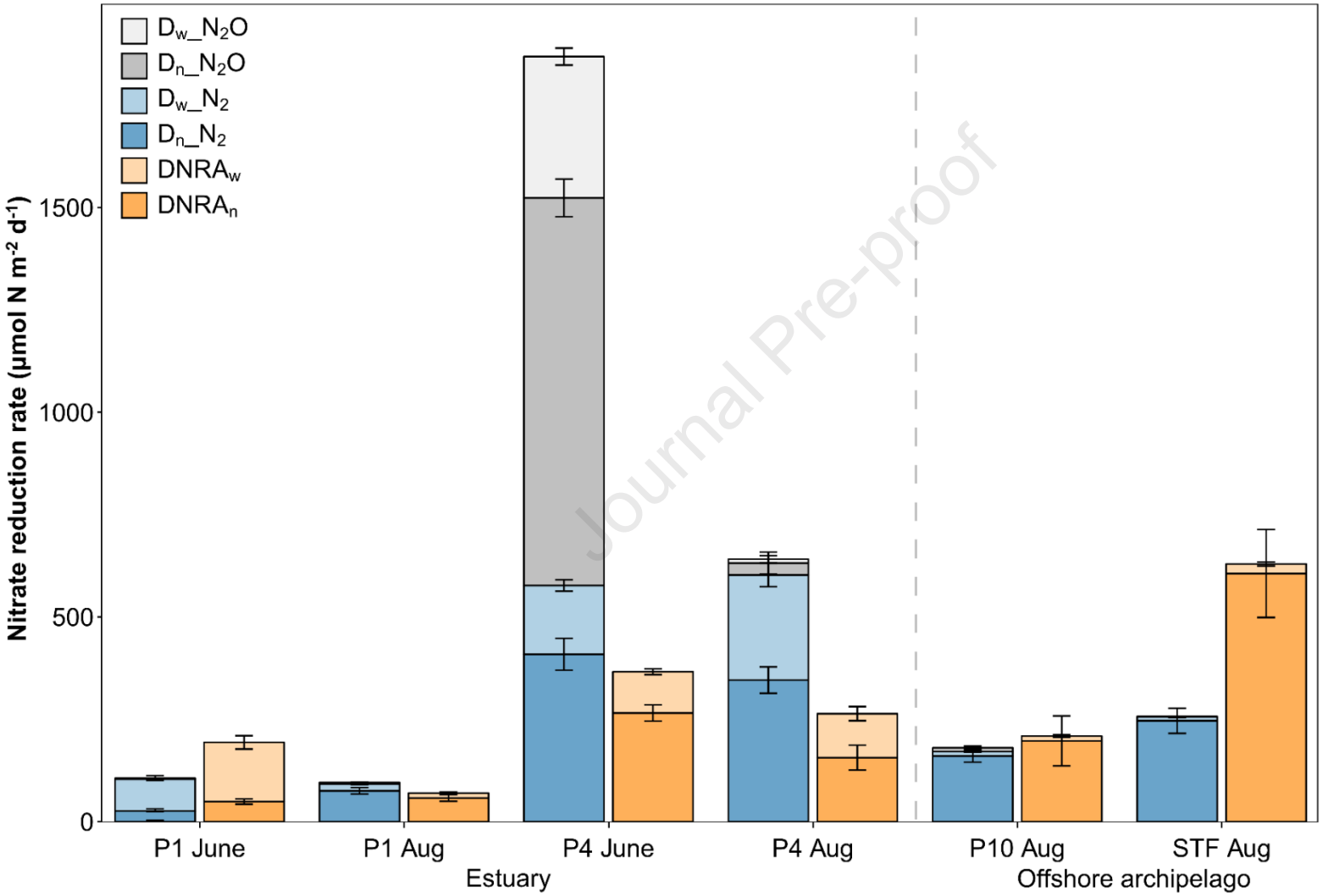

298

Figure 5. Differences in the a) absolute and b) relative rates of DNRA, and the proportion of N_2O of c) total nitrate reduction, and d) originating from denitrification stage of total N_2O production during coupled nitrification-denitrification process between the estuary stations in June (left orange bar, n = 8) and August (right orange bar, n = 8) and at the offshore archipelago stations in August (n = 8). Mean values ± standard deviation for estuary and offshore archipelago groups are given. The two groups are significantly different for each variable (one-way ANOVA/Mann-Whitney U test, $p < 0.05$).

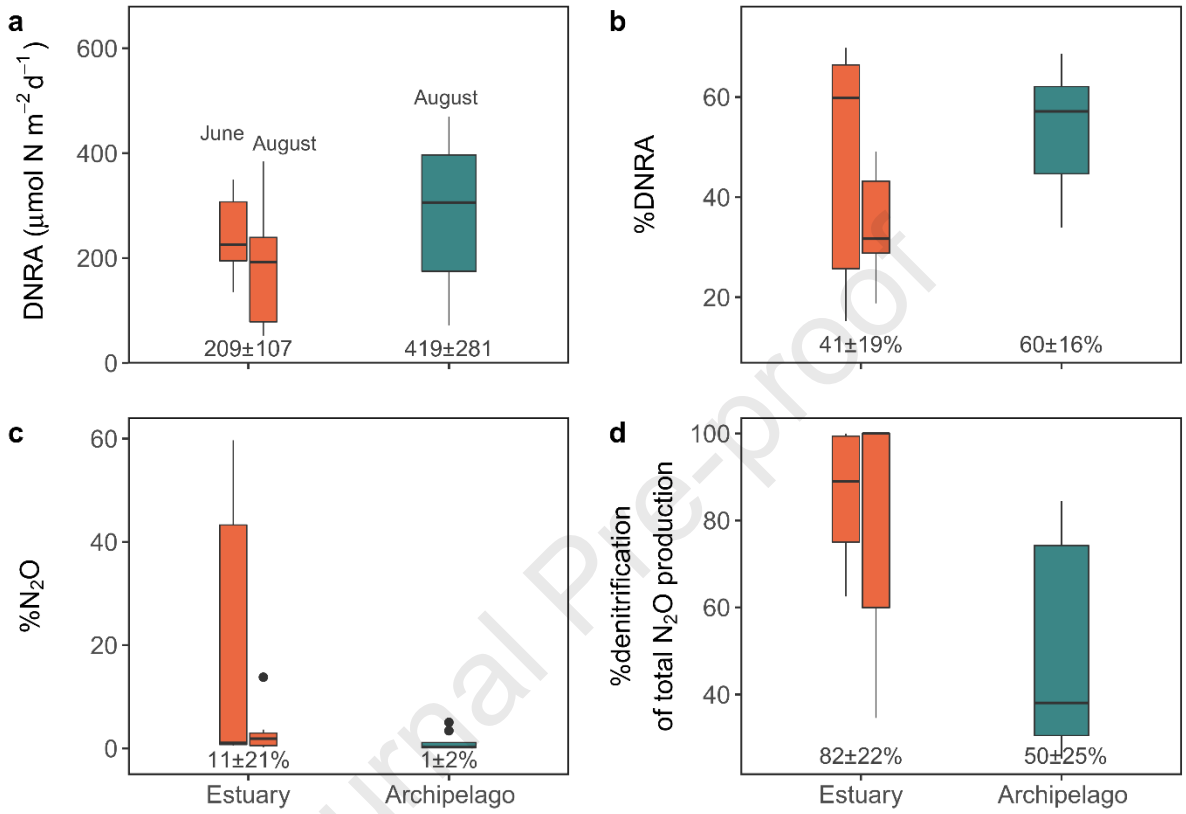

Figure 6. Relationships between dissolved organic carbon (DOC) and relative a) DNRA and b) N_2O production, and between bioavailable organic matter fraction (protein-like fluorescence; peak T) and relative c) DNRA and d) N_2O production at the estuary and offshore archipelago stations. The linear regression equations of the significant ($p < 0.05$) relationships only are presented.

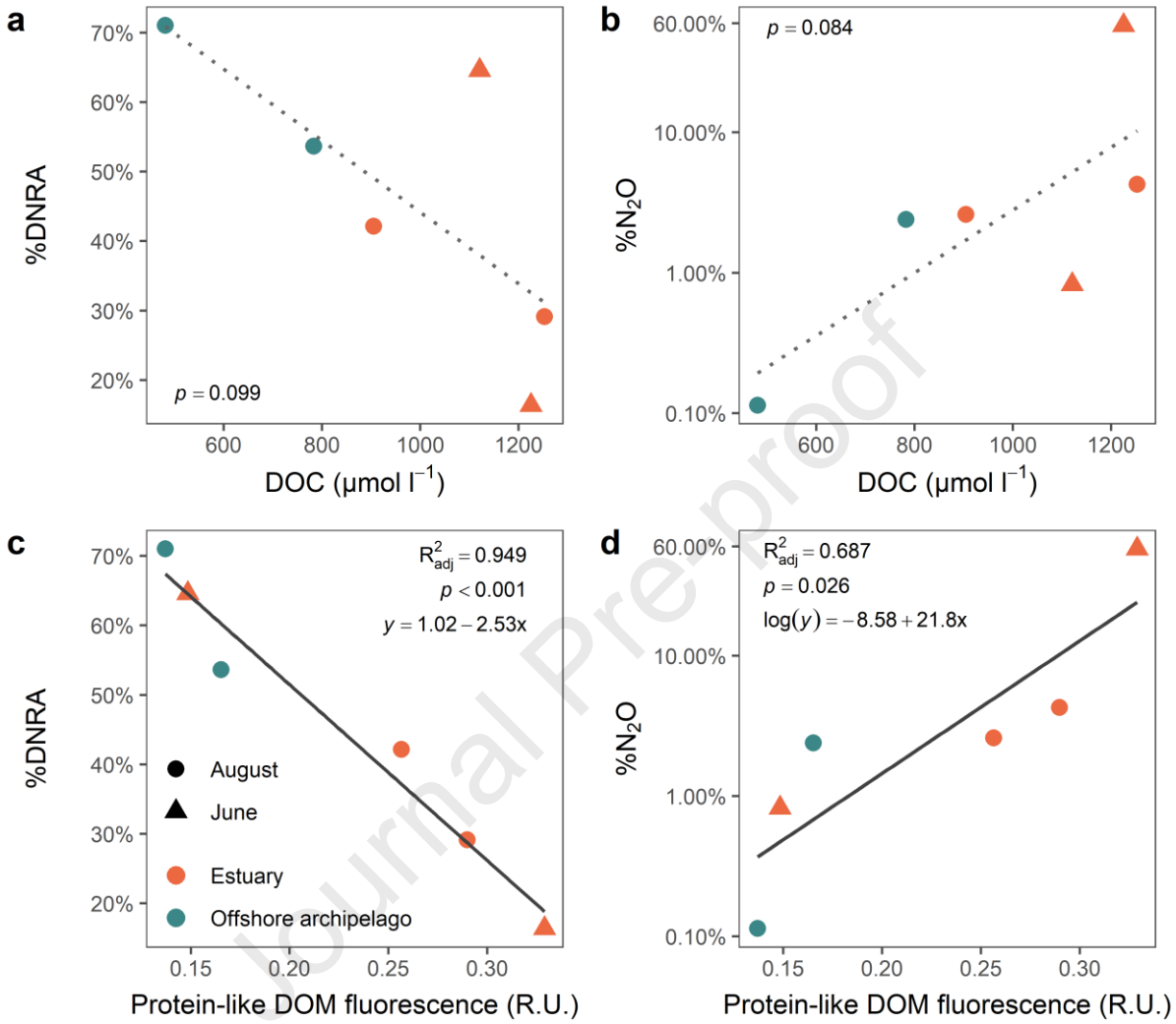

4 Discussion

Our results show that the dominant microbial nitrate reduction process switched from N-removing denitrification to N-recycling DNRA when moving from the terrestrially-dominated estuary to offshore archipelago region. This can be explained by changes in both DIN concentrations and organic carbon bioavailability. As expected, nitrate concentrations were generally higher at the estuarine than at the offshore archipelago stations, due to the diminishing impact of high-DIN riverine water (Asmala et al., 2017). In parallel, we observed strong contrasts in the DOM characteristics between estuary and offshore archipelago. High humic-like fluorescence, humification index and $SUVA_{254}$ in porewater DOM at the estuarine stations indicate a pronounced terrestrial contribution to the DOM pool (Asmala et al., 2013). These proxies suggest low DOM bioavailability in these areas, while high $S_{275–295}$ and BIX values at the offshore archipelago stations indicate a higher contribution of recently produced autochthonous, likely more bioavailable DOM (Lee et al., 2018). A similar gradient in the source of sedimentary particulate OM was observed by Jilbert et al., (2018), where sedimentary N:C values of 0.05-0.06 (C:N of 17-20) observed in the estuary indicated a higher contribution of terrestrially sourced material, while in the offshore region, the N:C of 0.13-0.14 (C:N of 7-8) reflected the dominance of phytoplankton-derived material.

In previous studies, denitrification has been shown to decrease with decreasing water-column nitrate concentrations in the coastal Baltic Sea (Asmala et al., 2017). Our data show that rates of all nitrate reduction processes using water column nitrate ($D_w\_N_2$, $D_w\_N_2O$, $DNRA_w$) decrease from estuary to offshore archipelago (Suppl. Fig. 3). However, because total nitrate reduction was mainly based on the nitrate provided through nitrification rather than water column nitrate, total nitrate reduction rates ($\sum N_2 + \sum N_2O$ + DNRA) were not significantly different between estuary and offshore archipelago stations. We suggest that the low amount of bioavailable carbon was limiting denitrification in the estuary, whereas decreasing nitrate availability started to limit the process offshore archipelago. The low bioavailable organic carbon-to-nitrate ratio at the estuarine stations was reflected in the higher denitrification-to-DNRA ratio, whereas DNRA dominated nitrate reduction under high bioavailable carbon-to-nitrate ratio at the offshore archipelago stations. A preference of the sediment microbial community for DNRA under nitrate-limited conditions has previously been explained in terms of the efficiency with which DNRA makes use of nitrate as an electron acceptor, with a higher rate of electron transfer per mole of N reduced despite the higher free energy yield of denitrification (Algar and Vallino, 2014). Interestingly, the DOM characteristics was directly related to N processes, while the amount of bulk organic carbon (as indicated by the porewater DOC concentration) was not (Fig. 6). We acknowledge that several alternative factors may

346 influence rates and pathways of nitrate reduction processes in coastal sediments. For instance, the
347 presence of hydrogen sulfide (H_2S) close to the sediment-water interface promotes %DNRA
348 (Plummer et al., 2015). However, upper-sediment sulfide concentrations in the range of 1–3 mM are
349 required for a clear impact on N processes, while sulfide in the upper sediments of our study area
350 were consistently < 0.1 mM (Jilbert et al., 2018). These low concentrations result from the titrating
351 effect of sedimentary Fe oxides in the coastal Baltic Sea, suggesting that sulfide is a minor driver of
352 the observed changes in %DNRA in our dataset. Furthermore, the presence of abundant Fe oxides
353 producing Fe^{2+}, an alternative electron donor, may promote DNRA (Kessler et al., 2018; Robertson et
354 al., 2016). Again, our study area shows only mild enrichments of porewater Fe^{2+} in the upper
355 sediments (up to 0.2 mM, Jilbert et al., 2018) in comparison to the sites studied by Robertson et al.,
356 (2016) (up to 0.8 mM), decreasing the potential significance of Fe. The anomalously high rates of
357 DNRA at P1 in June may however relate to porewater Fe^{2+}, since this is the most Fe-rich of our
358 sampling stations (see Station A in Jilbert et al., 2018).

359 In addition, our results demonstrate that the overall difference in potential organic carbon
360 bioavailability between estuary and offshore archipelago regions is likely to influence the end-
361 product of denitrification. At the near-shore estuarine stations, denitrification produced high
362 proportions of N_2O (1-58% of total nitrate reduction; 3-1230 µM N m^{-2} d^{-1}). This result implies that
363 nitrate was preferred over N_2O as an electron acceptor under conditions of high nitrate to
364 bioavailable carbon the nitrate-replete conditions of the estuary (Richardson et al., 2009), allowing
365 N_2O to accumulate in bottom waters. In contrast, the share of N_2O in denitrification was lower in the
366 offshore archipelago stations (0.1-2%, 1-9 µmol N m^{-2} d^{-1}), where the bulk carbon concentrations
367 were low but the contribution of bioavailable autochthonous carbon to the carbon pool was high
368 and nitrate concentration low. In accordance, N_2O concentrations in the bulk water column samples
369 collected between 2015 and 2017 were higher at the estuarine stations than in the offshore
370 archipelago, agreeing with the previous results in coastal environments with high freshwater impact
371 and fluctuating environmental conditions (e.g. Foster and Fulweiler, 2016; Nielsen et al., 2009;
372 Silvennoinen et al., 2008). While part of the accumulated N_2O can originate from nitrification or
373 coupled nitrification-denitrification (Foster and Fulweiler, 2016), we measured rather equal rates of
374 sediment nitrification at the estuary and offshore archipelago stations (estuary: 841±378, offshore
375 archipelago: 1089±193 µmol N m^{-2} d^{-1}; data not shown), arguing against an important role for
376 nitrification in N_2O production in the estuary. Furthermore, our data show that N_2O produced in
377 coupled nitrification-denitrification was mainly derived from denitrification. Although part of the
378 water-column N_2O pool in the estuary is likely advected with riverine water (Bange et al., 1998), the

majority appears to derive from sediment processes, since N_2O concentrations were generally higher in the bottom water than at the surface (Fig. 2).

Coastal systems are considered as important nutrient filters, reducing N loading from catchment areas towards the open sea. Although our results confirm that the main N removal process in the studied coastal environment is N_2-producing heterotrophic denitrification, they also highlight the importance of N-recycling DNRA. In the outer offshore archipelago region with decreasing influence of riverine water, DNRA can produce substantial amounts of bioavailable ammonium, enhancing the N recycling between sediments and surface water, especially in summer with the highest autochthonous biomass production and sedimentation. Intensifying eutrophication increases bioavailable carbon availability through higher algal biomass production, which in turn may promote DNRA and increase the role of estuaries as hotspots for N recycling, over N removal. This phenomenon has already been observed in some eutrophied systems (Bernard et al., 2015; Song et al., 2014), and could delay the recovery of water quality of the open sea in the Baltic Sea region.

The future role of eutrophic coastal systems as sources of N_2O to the atmosphere depends on the balance of N processes in coastal sediments. In systems such as Pohjanpitäjänlahti, the DIN pool of the estuary is dominated by nitrate, favouring production of N_2O during denitrification under nitrate-replete conditions. Hence, further increases in nutrient loading to this system is likely to enhance N_2O-producing denitrification, especially under scenarios of increased annual runoff and higher summer temperature, which will enhance stratification and hypoxia throughout the Baltic Sea (Meier et al., 2011), contributing to the predicted rise in emissions of this greenhouse gas in the future (Murray et al., 2015). Our results highlight the need to consider the intricate balance of processes in the nitrogen cycle along coastal gradients, especially in relation to organic carbon characteristics. Also their spatial variation and temporal evolution needs to be further clarified in order to properly understand the role of coastal ecosystems as filters of land-to-sea transfer of N.

5 Acknowledgements

We are grateful to the technical staff of Tvärminne Zoological Station and the Ecosystems and Environment Research Program at University of Helsinki for assistance during fieldwork and laboratory analyses. This work was supported by the Academy of Finland (projects 267112, 309748, 310302, and 317684)

6 References

Algar, C.K., Vallino, J.J., 2014. Predicting microbial nitrate reduction pathways in coastal sediments. Aquat. Microb. Ecol. 71, 223–238. https://doi.org/10.3354/ame01678

411 Asmala, E., Autio, R., Kaartokallio, H., Pitkänen, L., Stedmon, C.A., Thomas, D.N., 2013. Bioavailability
412 of riverine dissolved organic matter in three Baltic Sea estuaries and the effect of catchment
413 land use. Biogeosciences 10, 6969–6986. https://doi.org/10.5194/bg-10-6969-2013

414 Asmala, E., Carstensen, J., Conley, D.J., Slomp, C.P., Stadmark, J., Voss, M., 2017. Efficiency of the
415 coastal filter: Nitrogen and phosphorus removal in the Baltic Sea. Limnol. Oceanogr. 62, S222–
416 S238. https://doi.org/10.1002/lno.10644

417 Asmala, E., Haraguchi, L., Markager, S., Massicotte, P., Riemann, B., Staehr, P.A., Carstensen, J., 2018.
418 Eutrophication Leads to Accumulation of Recalcitrant Autochthonous Organic Matter in Coastal
419 Environment. Global Biogeochem. Cycles 32, 1673–1687.
420 https://doi.org/10.1029/2017GB005848

421 Bange, H.W., Dahlke, S., Ramesh, R., Meyer-Reil, L.A., Rapsomanikis, S., Andreae, M.O., 1998.
422 Seasonal study of methane and nitrous oxide in the coastal waters of the southern Baltic Sea.
423 Estuar. Coast. Shelf Sci. 47, 807–817. https://doi.org/10.1006/ecss.1998.0397

424 Barnes, R.T., Smith, R.L., Aiken, G.R., 2012. Linkages between denitrification and dissolved organic
425 matter quality, Boulder Creek watershed, Colorado. J. Geophys. Res. Biogeosciences 117, 1–14.
426 https://doi.org/10.1029/2011JG001749

427 Bernard, R.J., Mortazavi, B., Kleinhuizen, A.A., 2015. Dissimilatory nitrate reduction to ammonium
428 (DNRA) seasonally dominates NO3− reduction pathways in an anthropogenically impacted sub-
429 tropical coastal lagoon. Biogeochemistry 125, 47–64. https://doi.org/10.1007/s10533-015-
430 0111-6

431 Bonaglia, S., Deutsch, B., Bartoli, M., Marchant, H.K., Brüchert, V., 2014. Seasonal oxygen, nitrogen
432 and phosphorus benthic cycling along an impacted Baltic Sea estuary: Regulation and spatial
433 patterns. Biogeochemistry 119, 139–160. https://doi.org/10.1007/s10533-014-9953-6

434 Bouwman, A.F., Bierkens, M.F.P., Griffioen, J., Hefting, M.M., Middelburg, J.J., Middelkoop, H.,
435 Slomp, C.P., 2013. Nutrient dynamics, transfer and retention along the aquatic continuum from
436 land to ocean: Towards integration of ecological and biogeochemical models. Biogeosciences
437 10, 1–23. https://doi.org/10.5194/bg-10-1-2013

438 Burdige, D.J., 2006. Geochemistry of Marine Sediments, 1st ed. Princeton Univ. Press, Princeton.

439 Carlson, H.K., Lui, L.M., Price, M.N., Kazakov, A.E., Carr, A. V., Kuehl, J. V., Owens, T.K., Nielsen, T.,
440 Arkin, A.P., Deutschbauer, A.M., 2020. Selective carbon sources influence the end-products of
441 microbial nitrate respiration. ISME J. https://doi.org/10.1038/s41396-020-0666-7

Christensen, P.B., Rysgaard, S., Sloth, N.P., Dalsgaard, T., Schwærter, S., 2000. Sediment mineralization, nutrient fluxes, denitrification and dissimilatory nitrate reduction to ammonium in an estuarine fjord with sea cage trout farms. Aquat. Microb. Ecol. 21, 73–84. https://doi.org/10.3354/ame021073

Coble, P.G., 1996. Characterization of marine and terrestrial DOM in seawater using excitation-emission matrix spectroscopy. Mar. Chem. 51, 325–346. https://doi.org/10.1016/0304-4203(95)00062-3

Dong, L.F., Nedwell, D.B., Stott, A., 2006. Sources of nitrogen used for denitrification and nitrous oxide formation in sediments of the hypernutrified Colne, the nutrified Humber, and the oligotrophic Conwy estuaries, United Kingdom. Limnol. Oceanogr. 51, 545–557. https://doi.org/10.4319/lo.2006.51.1_part_2.0545

Fellman, J.B., Petrone, K.C., Grierson, P.F., 2011. Source, biogeochemical cycling, and fluorescence characteristics of dissolved organic matter in an agro-urban estuary. Limnol. Oceanogr. 56, 243–256. https://doi.org/10.4319/lo.2011.56.1.0243

Foster, S.Q., Fulweiler, R.W., 2016. Sediment nitrous oxide fluxes are dominated by uptake in a temperate estuary. Front. Mar. Sci. 3, 1–13. https://doi.org/10.3389/fmars.2016.00040

Giblin, A.E., Tobias, C.R., Song, B., Weston, N., Banta, G.T., Rivera-Monroy, V.H., 2013. The importance of dissimilatory nitrate reduction to ammonium (DNRA) in the nitrogen cycle of coastal ecosystems. Oceanography 26, 124–131. https://doi.org/10.5670/oceanog.2013.54

Goñi, M.A., Teixeira, M.J., Perkeya, D.W., 2003. Sources and distribution of organic matter in a river-dominated estuary (Winyah Bay, SC, USA). Estuar. Coast. Shelf Sci. 57, 1023–1048. https://doi.org/10.1016/S0272-7714(03)00008-8

Hardison, A.K., Algar, C.K., Giblin, A.E., Rich, J.J., 2015. Influence of organic carbon and nitrate loading on partitioning between dissimilatory nitrate reduction to ammonium (DNRA) and N2 production. Geochim. Cosmochim. Acta 164, 146–160. https://doi.org/10.1016/j.gca.2015.04.049

Heiskanen, A.S., Kononen, K., 1994. Sedimentation of vernal and late summer phytoplankton communities in the coastal Baltic Sea. Arch. fur Hydrobiol. 131, 175–198.

Hellemann, D., Tallberg, P., Aalto, S.L., Bartoli, M., Hietanen, S., 2020. Seasonal cycle of benthic denitrification and DNRA in the aphotic coastal zone, northern Baltic Sea. Mar. Ecol. Prog. Ser. 637, 15–28.

473 Hellemann, D., Tallberg, P., Bartl, I., Voss, M., Hietanen, S., 2017. Denitrification in an oligotrophic
474 estuary: A delayed sink for riverine nitrate. Mar. Ecol. Prog. Ser. 583, 63–80.
475 https://doi.org/10.3354/meps12359

476 Hietanen, S., 2007. Anaerobic ammonium oxidation (anammox) in sediments of the Gulf of Finland.
477 Aquat. Microb. Ecol. 48, 197–205. https://doi.org/10.3354/ame048197

478 Hietanen, S., Kuparinen, J., 2008. Seasonal and short-term variation in denitrification and anammox
479 at a coastal station on the Gulf of Finland, Baltic Sea. Hydrobiologia 596, 67–77.
480 https://doi.org/10.1007/s10750-007-9058-5

481 Huguet, A., Vacher, L., Relexans, S., Saubusse, S., Froidefond, J.M., Parlanti, E., 2009. Properties of
482 fluorescent dissolved organic matter in the Gironde Estuary. Org. Geochem. 40, 706–719.
483 https://doi.org/10.1016/j.orggeochem.2009.03.002

484 Jilbert, T., Asmala, E., Schröder, C., Tiihonen, R., Myllykangas, J.P., Virtasalo, J.J., Kotilainen, A.,
485 Peltola, P., Ekholm, P., Hietanen, S., 2018. Impacts of flocculation on the distribution and
486 diagenesis of iron in boreal estuarine sediments. Biogeosciences 15, 1243–1271.
487 https://doi.org/10.5194/bg-15-1243-2018

488 Kessler, A.J., Roberts, K.L., Bissett, A., Cook, P.L.M., 2018. Biogeochemical Controls on the Relative
489 Importance of Denitrification and Dissimilatory Nitrate Reduction to Ammonium in Estuaries.
490 Global Biogeochem. Cycles 32, 1045–1057. https://doi.org/10.1029/2018GB005908

491 Kraft, B., Tegetmeyer, H.E., Sharma, R., Klotz, M.G., Ferdelman, T.G., Hettich, R.L., Geelhoed, J.S.,
492 Strous, M., 2014. The environmental controls that govern the end product of bacterial nitrate
493 respiration. Science (80-.). 345, 676–679. https://doi.org/10.1126/science.1254070

494 Lee, M.H., Osburn, C.L., Shin, K.H., Hur, J., 2018. New insight into the applicability of spectroscopic
495 indices for dissolved organic matter (DOM) source discrimination in aquatic systems affected
496 by biogeochemical processes. Water Res. 147, 164–176.
497 https://doi.org/10.1016/j.watres.2018.09.048

498 Malve, O., Virtanen, M., Villa, L., Karonen, M., Aakerla, H., Heiskanen, A.S., Lappalainen, K.M.,
499 Holmberg, R., 2000. Artificial oxygenation experiment in hypolimnion of Pojo Bay estuary in
500 1995 and 1996: Factors regulating estuary circulation and oxygen and salt balances. Finnish
501 Environ. 377, 1-163 (In Finnish with English summary).

502 Massicotte, P., 2018. eemR: Tools for Pre-Processing Emission-Excitation-Matrix (EEM) Fluorescence
503 Data. R package version 1.0.1. https://CRAN.R-project.org/package=eemR.

504 Mattsson, T., Kortelainen, P., Räike, A., 2005. Export of DOM from boreal catchments: Impacts of
505 land use cover and climate. Biogeochemistry 76, 373–394. https://doi.org/10.1007/s10533-
506 005-6897-x

507 Meier, H.E.M., Andersson, H.C., Eilola, K., Gustafsson, B.G., Kuznetsov, I., Mller-Karulis, B., Neumann,
508 T., Savchuk, O.P., 2011. Hypoxia in future climates: A model ensemble study for the Baltic Sea.
509 Geophys. Res. Lett. 38, 1–6. https://doi.org/10.1029/2011GL049929

510 Murphy, K.R., Stedmon, C.A., Waite, T.D., Ruiz, G.M., 2008. Distinguishing between terrestrial and
511 autochthonous organic matter sources in marine environments using fluorescence
512 spectroscopy. Mar. Chem. 108, 40–58. https://doi.org/10.1016/j.marchem.2007.10.003

513 Murray, R.H., Erler, D. V., Eyre, B.D., 2015. Nitrous oxide fluxes in estuarine environments: Response
514 to global change. Glob. Chang. Biol. 21, 3219–3245. https://doi.org/10.1111/gcb.12923

515 Myllykangas, J.P., Jilbert, T., Jakobs, G., Rehder, G., Werner, J., Hietanen, S., 2017. Effects of the 2014
516 major Baltic inflow on methane and nitrous oxide dynamics in the water column of the central
517 Baltic Sea. Earth Syst. Dyn. 8, 817–826. https://doi.org/10.5194/esd-8-817-2017

518 Nielsen, L.P., 1992. Denitrification in sediment determined from nitrogen isotope pairing. FEMS
519 Microbiol. Lett. 86, 357–362. https://doi.org/10.1111/j.1574-6968.1992.tb04828.x

520 Nielsen, M., Gieseke, A., De Beer, D., Revsbech, N.P., 2009. Nitrate, nitrite, and nitrous oxide
521 transformations in sediments along a salinity gradient in the Weser Estuary. Aquat. Microb.
522 Ecol. 55, 39–52. https://doi.org/10.3354/ame01275

523 Plummer, P., Tobias, C., Cady, D., 2015. Nitrogen reduction pathways in estuarine sediments:
524 Influences of organic carbon and sulfide. J. Geophys. Res. Biogeosciences 120, 1958–1972.
525 https://doi.org/10.1002/2015JG003004.Received

526 R Core Team, 2020. R: A language and environment for statistical computing.

527 Räike, A., Kortelainen, P., Mattsson, T., Thomas, D.N., 2012. 36year trends in dissolved organic
528 carbon export from Finnish rivers to the Baltic Sea. Sci. Total Environ. 435–436, 188–201.
529 https://doi.org/10.1016/j.scitotenv.2012.06.111

530 Richardson, D., Felgate, H., Watmough, N., Thomson, A., Baggs, E., 2009. Mitigating release of the
531 potent greenhouse gas N2O from the nitrogen cycle - could enzymic regulation hold the key?
532 Trends Biotechnol. 27, 388–397. https://doi.org/10.1016/j.tibtech.2009.03.009

533 Risgaard-Petersen, N., Revsbech, N.P., Rysgaard, S., 1995. Combined microdiffusion-hypobromite

534 oxidation method for determining nitrogen-15 isotope in ammonium. Soil Sci. Soc. Am. J. 59,
535 1077–1080.

536 Robertson, E.K., Roberts, K.L., Burdorf, L.D.W., Cook, P., Thamdrup, B., 2016. Dissimilatory nitrate
537 reduction to ammonium coupled to Fe(II) oxidation in sediments of a periodically hypoxic
538 estuary. Limnol. Oceanogr. 61, 365–381. https://doi.org/10.1002/lno.10220

539 Silvennoinen, H., Liikanen, A., Torssonen, J., Stange, C.F., Martikainen, P.J., 2008. Denitrification and
540 N2O effluxes in the Bothnian Bay (northern Baltic Sea) river sediments as affected by
541 temperature under different oxygen concentrations. Biogeochemistry 88, 63–72.
542 https://doi.org/10.1007/s10533-008-9194-7

543 Song, B., Lisa, J.A., Tobias, C.R., 2014. Linking DNRA community structure and activity in a shallow
544 lagoonal estuarine system. Front. Microbiol. 5, 1–10.
545 https://doi.org/10.3389/fmicb.2014.00460

546 Spencer, R.G.M., Ahad, J.M.E., Baker, A., Cowie, G.L., Ganeshram, R., Upstill-Goddard, R.C., Uher, G.,
547 2007. The estuarine mixing behaviour of peatland derived dissolved organic carbon and its
548 relationship to chromophoric dissolved organic matter in two North Sea estuaries (U.K.).
549 Estuar. Coast. Shelf Sci. 74, 131–144. https://doi.org/10.1016/j.ecss.2007.03.032

550 Stelzer, R.S., Thad Scott, J., Bartsch, L.A., Parr, T.B., 2014. Particulate organic matter quality
551 influences nitrate retention and denitrification in stream sediments: Evidence from a carbon
552 burial experiment. Biogeochemistry 119, 387–402. https://doi.org/10.1007/s10533-014-9975-0

553 Thamdrup, B., Dalsgaard, T., 2002. Production of N2 through anaerobic ammonium oxidation
554 coupled to nitrate reduction in marine sediments. Appl. Environ. Microbiol. 68, 1312–1318.
555 https://doi.org/10.1128/AEM.68.3.1312

556 Zhao, Y., Xia, Y., Li, B., Yan, X., 2014. Influence of environmental factors on net N2 and N2O
557 production in sediment of freshwater rivers. Environ. Sci. Pollut. Res. 21, 9973–9982.
558 https://doi.org/10.1007/s11356-014-2908-6

559 Zsolnay, A., Baigar, E., Jimenez, M., Steinweg, B., Saccomandi, F., 1999. Differentiating with
560 fluorescence spectroscopy the sources of dissolved organic matter in soils subjected to drying.
561 Chemosphere 38, 45–50. https://doi.org/10.1016/S0045-6535(98)00166-0

562

Highlights

- The availability of bioavailable carbon defines nitrate reduction end-product
- Estuaries with low bioavailable organic carbon can release high amounts of N2O
- Nitrogen is recycled through DNRA in the archipelago areas

Aalto et al.

Author statement

Sanni L. Aalto: Methodology, Formal analysis, Investigation, Writing - Original Draft, Writing - Review & Editing, Visualization

Eero Asmala: Methodology, Formal analysis, Investigation, Writing - Review & Editing, Visualization

Tom Jilbert: Methodology, Investigation, Resources, Writing - Review & Editing, Visualization

Susanna Hietanen: Conceptualization, Methodology, Investigation, Resources, Supervision, Funding acquisition

Declaration of interests

☒ The authors declare that they have no known competing financial interests or personal relationships that could have appeared to influence the work reported in this paper.

☐The authors declare the following financial interests/personal relationships which may be considered as potential competing interests: